JOURNAL OF SOLID STATE CHEMISTRY 19, 179–192 (1976)

Direct Lattice Imaging of Polytypes in YSeF

D. VAN DYCK, J. VAN LANDUYT, AND S. AMELINCKX*

Rijksuniversitair Centrum Antwerpen, Middelheimlaan 1, 2020 Antwerpen, Belgium

NGUYEN HUY-DUNG AND CHRISTIAN DAGRON

Faculté des sciences pharmaceutiques et biologiques, 4 avenue de l'Observatoire 75006 Paris, France

Received June 15, 1976

High-resolution imaging was used to study a series of different YSeF polytypes. By comparing the images with the known structures of a few of them that had previously been characterized by X-ray diffraction, an imaging code could be derived which allows one to deduce the structures of the other polytypes from their lattice images. Mixtures of polytypes and, in some cases, frozen-in defects associated with their formation could be identified. Optical simulation of the electron diffraction patterns by means of simplified polytype models shows a fairly good agreement with the electron diffraction patterns and provides a complementary tool for the identification of the polytypes especially in those cases where no lattice images could be obtained.

Introduction

In the course of a systematic study of lanthanide compounds with two different anions, by means of X-ray diffraction techniques, Dagron (*1*) demonstrated the existence of a very characteristic polytypism in YSeF. Eight different polytypes could be distinguished. Their unit-cell parameters obey simple geometrical relations according to which they can be subdivided into an orthorhombic and a monoclinic class with the same a and c parameters.

Nguyen Huy-Dung was able to determine the crystal structure of three polytypes (*2–4*) by Patterson analysis, refined by a least-squares method. These polytypes were found to be built up by the periodic stacking of two types of unit blocks, called S and T hereafter. These unit blocks have the same a and b parameters but the enclosed angles are each other's supplements.

The application of the X-ray technique to determine the structure of the remaining polytypes is very difficult due to the fact that their preparation in the form of pure monocrystals is almost impossible. Besides, this technique is less adapted to the study of long and more complicated sequences. As opposed to X-ray diffraction, high-resolution electron microscopy is more suitable for the study of compounds with large unit cells and can also be applied to the investigation of less pure and polycrystalline materials. For these reasons direct imaging in electron microscopy can be used as a complementary tool for the study of the more complicated polytypes and of irregular sequences and defects.

In order to translate the images into the corresponding structures, an imaging code for the S and T blocks has to be deduced. This can be obtained by comparing the structures of the known polytypes with the images obtained viewing down the c-axis.

* Also at S.C.K.-C.E.N., 2400 Mol, Belgium.

Optical simulation of the diffraction pattern is also found to yield supplementary information for the identification of complex polytypes.

The Structure of YSeF Polytypes

In previous X-ray studies (*1*) eight polytypes could be distinguished on the basis of their unit cells, all having the same lattice parameters a and c:

$$a = 9.91 \text{ Å} \qquad c = 4.08 \text{ Å}.$$

According to their b and γ parameters they can further be subdivided into two classes:

(1) The *monoclinic series*, called M where the b and γ parameter obey the relations:

$$b = n\,b_o/\sin\gamma \qquad \text{with } b_o = 3.15 \text{ Å} \qquad (1)$$

and

$$b\cos\gamma = a/3.$$

Monoclinic polytypes corresponding to the n values 2, 4, 6, 8, 10, and 12 have been observed.

(2) The *orthorhombic series*, hereafter noted by O, obeys the relation

$$b = n\,b_o \qquad (2)$$

where n takes the values 2, 6, and 14.

A complete structure analysis by means of X-ray diffraction techniques was first carried out for three polytypes (those with small b parameters), i.e., 6 O, 2 O, and 4 M (*2–4*).

Only the general features of the structures, required for a proper understanding of the electron microscopic images will be given here. The structural description will in the first place be illustrated for the polytype 6 O because it shows more clearly the general stacking rules of the elementary building blocks. The projection of the structure of this orthorhombic polytype on the (a, b)-plane is represented in Fig. 1.

In the left part of the unit cell, two types of parallel planes containing the Y atoms can be distinguished. They are parallel to the c-axis, equidistant, and alternating, as illustrated in Fig. 1b.

The first type of plane contains only Y and F atoms, each F atom being located near the center of a triangle of Y atoms and every Y atom being surrounded by a hexagon of F atoms and by two Se atoms lying on either side of the plane; in Fig. 1b these are represented by double lines.

In the second type of plane, the Y atoms are octahedrally surrounded by the Se atoms lying between the two types of planes (Fig. 1a);

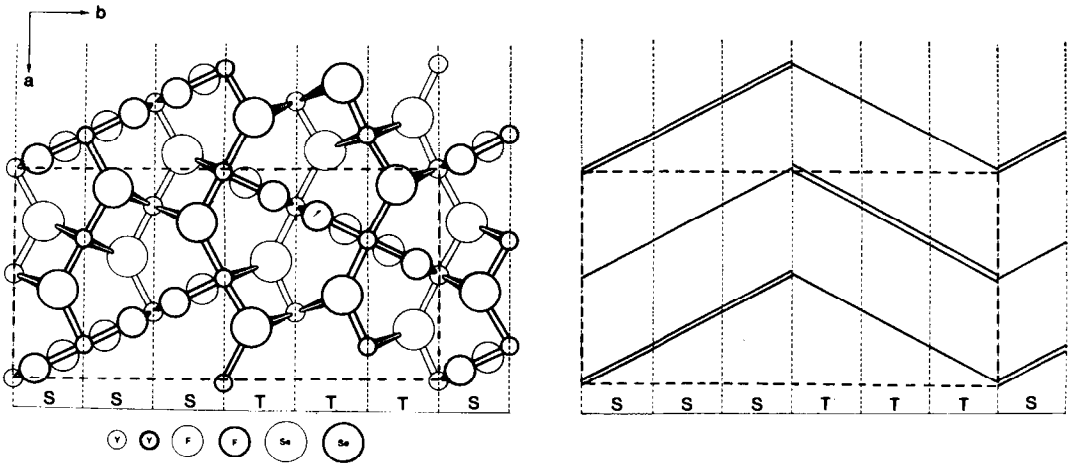

FIG. 1. Projection of the unit cell of the polytype 6 O on the (a, b)-plane. A schematic representation of the different Y-planes is given on the right where the double lines represent YF-planes and the single lines pure Y planes.

these planes are represented by single lines in Fig. 1b.

The angle γ between those planes and the a-axis

$$tg\,\gamma = a/b,$$

where a and b are the parameters of the orthorhombic unit cell. The distance along the a-axis between these two types of planes is $a/2$. As indicated in Fig. 1, the unit block, containing Y-planes with a slope rising from left to right is called S. Two types of S blocks can be distinguished; they can be deduced one from the other by a rotation about a twofold axis parallel to c. The right part of the unit cell shows the same Y-planes, but with downward slope. Such a unit block will be called T. The T blocks can also be deduced from the S blocks by the glide mirror operation (a, c) with translation vector $a/2$ along [100], consistent with the space group *Pnam* of this polytype. Hence the type of the Y-plane interchanges on passing through an S–T boundary, but it remains the same through an S–S or a T–T boundary. The polytype 6 O can thus be described by a periodic stacking of blocks following the sequence *SSSTTTSSSTTT*. . .. Throughout the rest of this paper, we will represent the Y-planes by the symbolism illustrated in Fig. 1b.

Figure 2 shows the projection of the unit cell of the orthorhombic type 2 O on the same (a, b)-plane. There also the S and T blocks

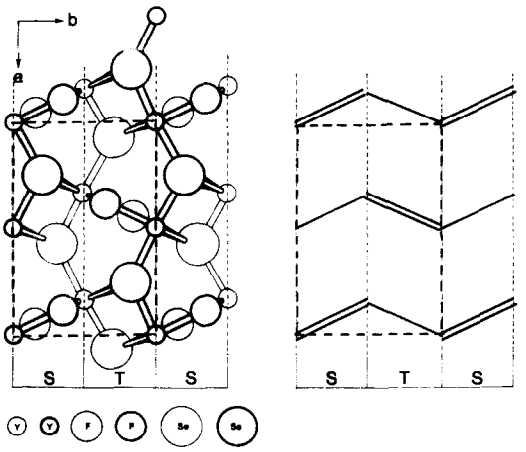

FIG. 2. Projection of the unit cell of the orthorhombic polytype 2 O on the (a, b)-plane. The same schematic representation as in Fig. 1 is given on the right of the figure.

can be observed, so that the polytype can be described as consisting of a repeated stacking of the block sequence *STST* . . ., which is also shown schematically in Fig. 2b. This polytype has the same spacegroup *Pnam*.

In Fig. 3 the projection of a unit cell of the monoclinic polytype 4 M on the (a, b)-plane is shown. This polytype is built up by the block sequence *SSSTSSST* which is monoclinic due to the unequal number of S and T blocks. The space group of this polytype is $P2_1/m$.

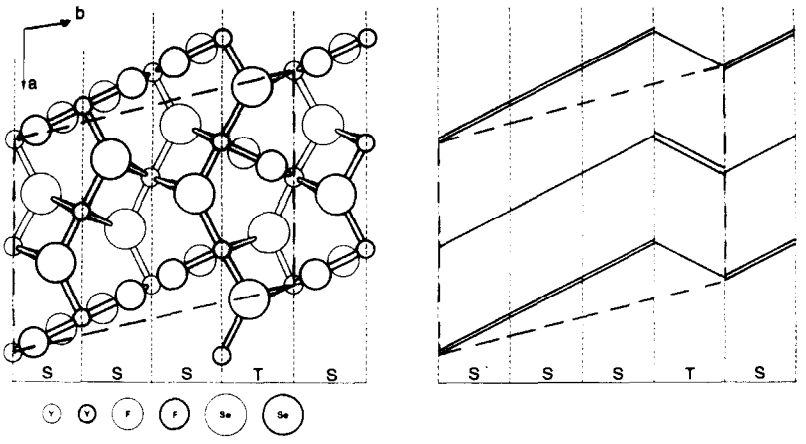

FIG. 3. (a, b) projection of the unit cell of the monoclinic polytype 4 M.

In general, it can be postulated that all of the YSeF polytypes are constructed by a repeated stacking of the two types of blocks called S and T. The width of the S and T blocks is $b_o = 3.15$ Å. The distance between similar types of Y-planes is $a_o = 9.91$ Å and their slope angle, i.e., the angle γ between the planes and the b-axis is given by $tg\ \gamma = a_o/(6b_o)$. Depending on whether the numbers of S and T blocks within one repeat distance are equal or unequal, the polytypes are orthorhombic (O) or monoclinic (M). Calling n the total number of blocks in this sequence, we can use the notation $n\ O$ or $n\ M$ as, e.g., 6 O, 12 M.

This model is consistent with Eqs. (1) and (2) obeyed by the unit-cell parameters of all the polytypes and is in agreement with the X-ray structures of the polytypes 6 O, 2 O, and 4 M.

At this point the direct lattice imaging technique of electron microscopy can be applied for testing the model on the other polytypes and for deducing their stacking sequence.

Experimental Methods

Specimen Preparation

A basic product was prepared by mixing Y_2Se_3 and YF_3 in stoichiometric proportions and sintering the mixture under argon pressure for 2 weeks at 800°C, followed by rapid quenching in liquid mercury at −30°C. The different polytypes are then obtained by annealing the product for 2 weeks at different but very accurately stabilized temperatures.

The temperatures at which the different polytypes are obtained are given in Table I.

Before examination by electron microscopy, a number of crystals were characterized by means of X-ray diffraction. Afterward the crystals were ground in an agate mortar, the powder was suspended in methanol, and a drop of the suspension was deposited on a thin perforated carbon film. Thin parts of well-oriented crystals, protruding over the border of a hole, could be used for direct imaging. In some cases, grinding was carried out at liquid nitrogen temperature where the material is more brittle and where cleavage along the required (a, b)-plane is favored.

Direct Imaging Technique

All high-resolution micrographs were taken with a JEOL 100C electron microscope equipped with a side-entry goniometer stage and a hairpin type filament. The point to point resolution was 5 Å. The primary magnification was 290,000×. The electron beam radiation damage was reduced by observing the samples as quickly as possible with minimum beam intensity. Astigmatism was corrected in the granular structure of the carbon microgrids. All the specimens were oriented so as to make the incident electron beam parallel to the c-axis, and all diffracted beams corresponding to interplanar spacing down to $\frac{1}{3}$ Å^{-1} were used for the image formation, as shown in Fig. 4. In this situation it was possible to obtain two-dimensional lattice images, related to the crystal structure. A complete through focus series was taken for several fragments of each sample. Exposure times between 3 and 5 sec were used. In order to enable the interpretation of the images using an "imaging code," all of the micrographs were taken in the thinnest crystal regions, under the same diffraction conditions and at the same underfocus (~1500 Å).

Optical Diffraction Simulation

On a simplified two-dimensional graphic model of the structure of the investigated

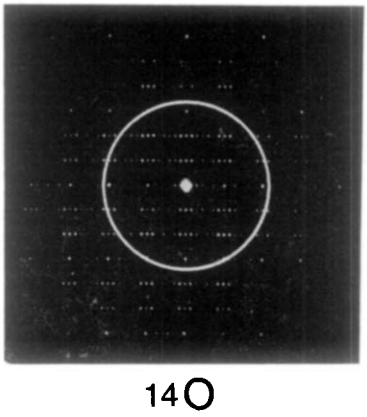

FIG. 4. Typical diffraction pattern of the polytype 14 O. The position and size of the aperture, including the beams contributing to the image formation are also indicated.

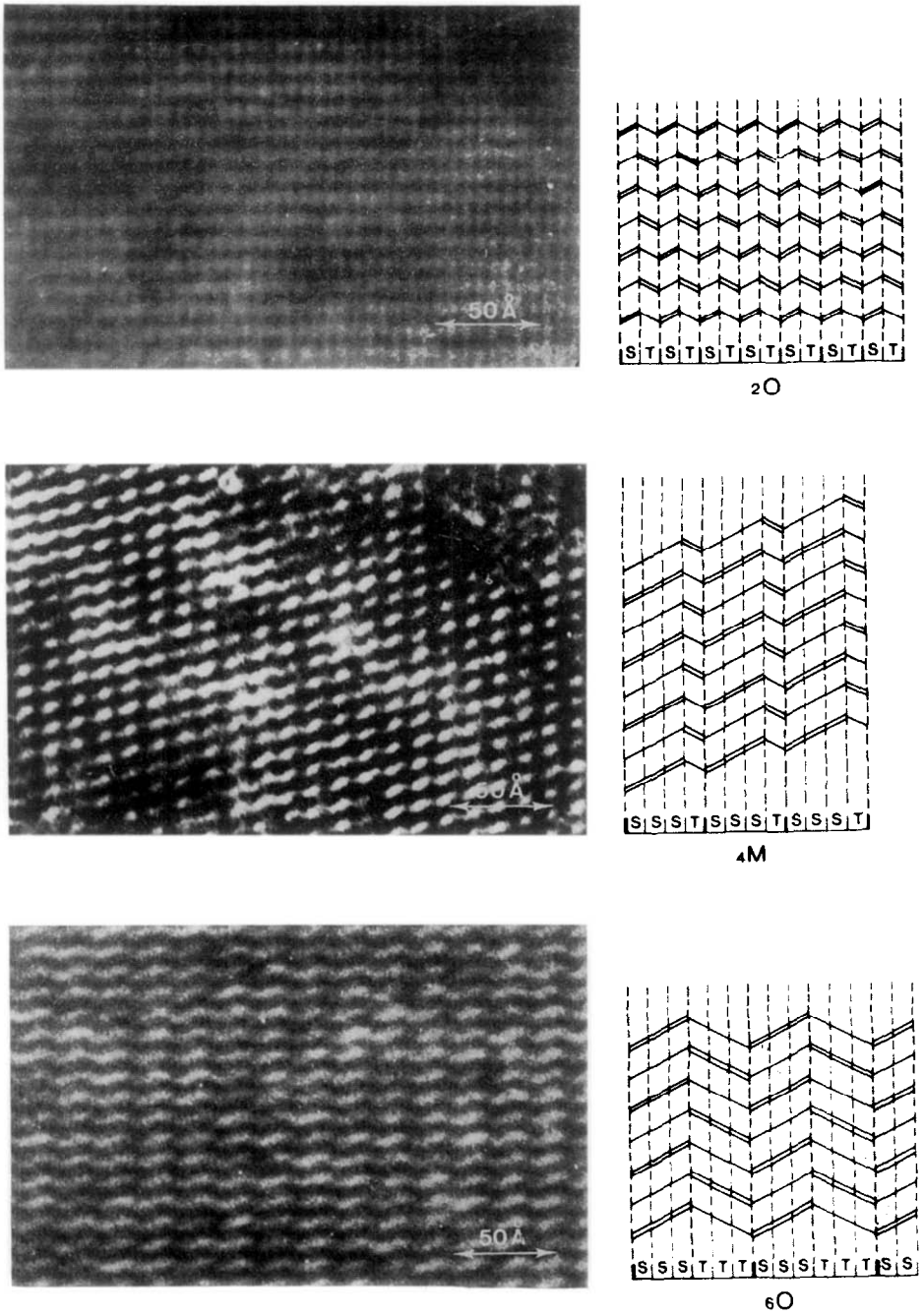

FIG. 5. Comparison of the lattice images of the polytypes 2 *O*, 4 *M*, and 6 *O* with their corresponding schematic projected structures. The stacking sequences (S-T-symbolism) are also indicated.

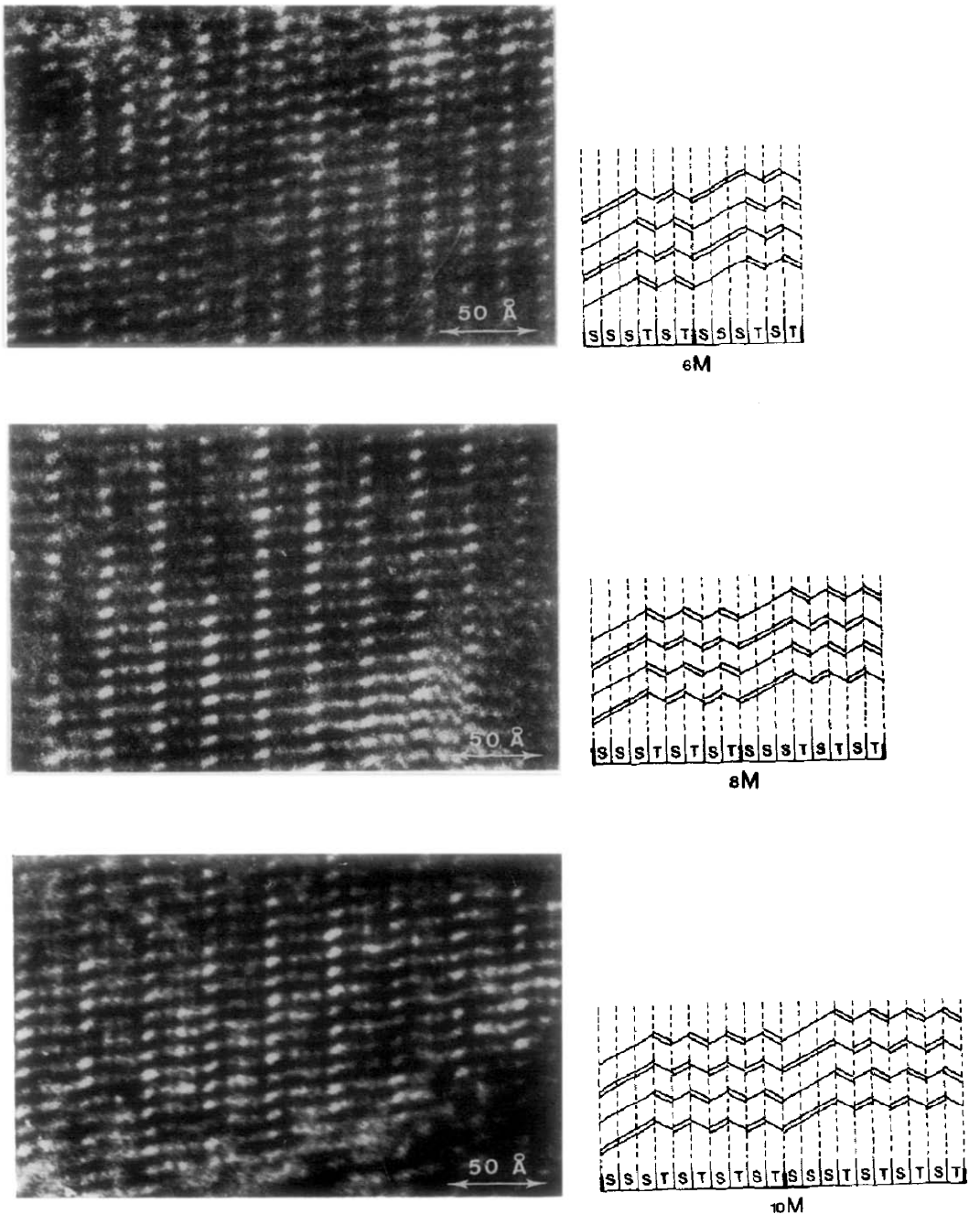

FIG. 6. Comparison of the lattice images of the polytypes 6 *M*, 8 *M*, and 10 *M* with their proposed structure in terms of *ST* stacking, as derived from the imaging code.

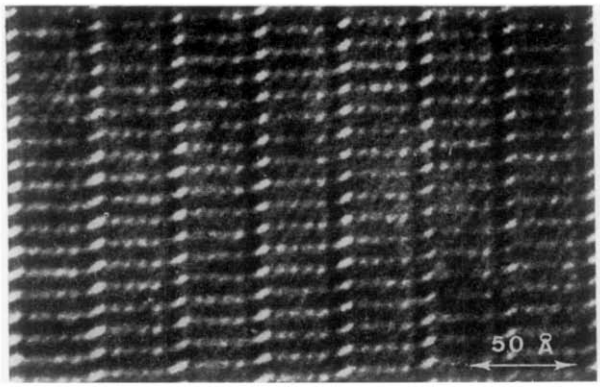

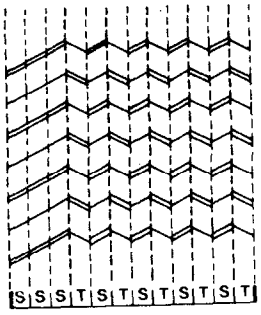

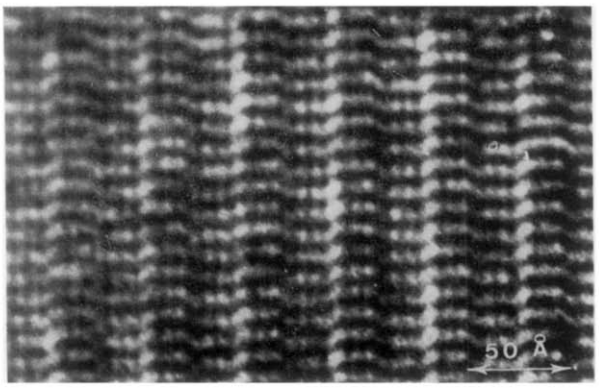

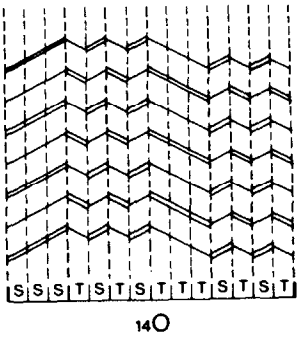

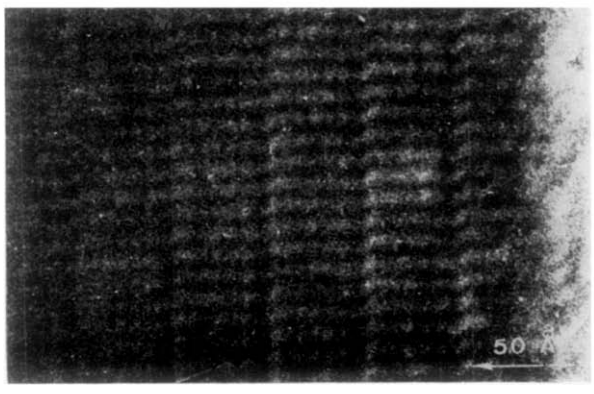

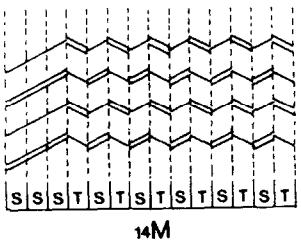

FIG. 7. Comparison of the lattice images of the polytypes 12 *M* 14 *O* and 14 *M*, with the proposed *ST* stackings, as derived from the imaging code.

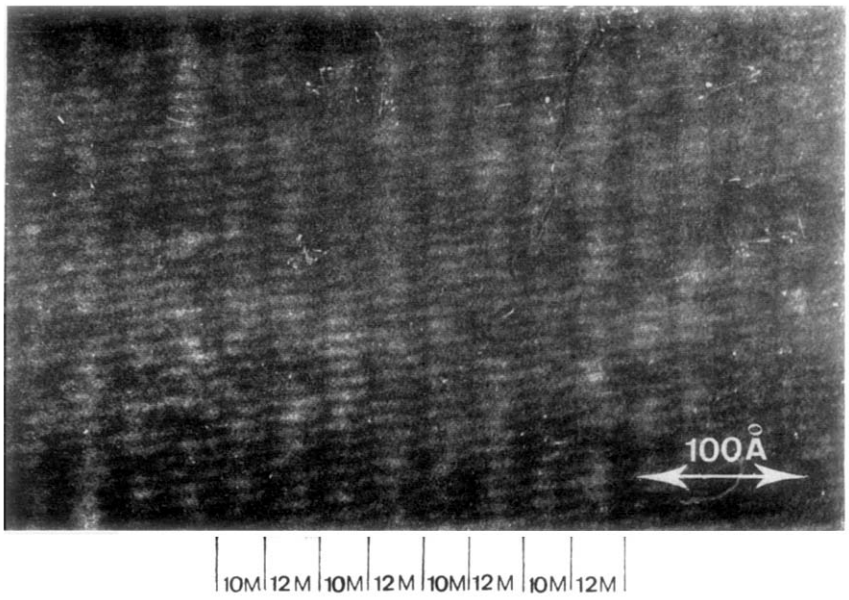

FIG. 8. Lattice image of the polytype (10 + 12) *M*. Alternating strips can be observed, respectively 32 and 38 Å in width.

polytype, the two types of Y-planes were drawn as lines with different thicknesses, chosen to be roughly proportional to the relative scattering power of the corresponding planes. Figure 9 shows, e.g., the model used for the optical diffraction simulation of the polytype 14 *O*.

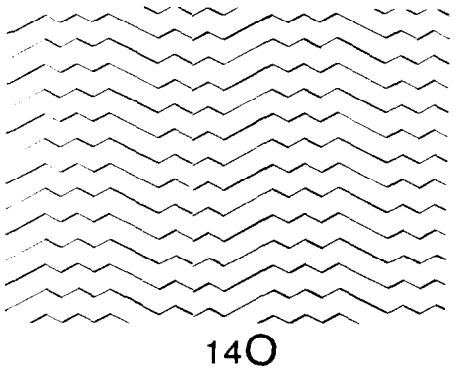

FIG. 9. Grating model used for diffraction simulation of the electron diffraction for the polytype 14 *O*.

Identical drawings were periodically arranged and photographically reduced to a size comparable with the wavelength of visible light. Such gratings were finally used to perform optical diffraction experiments using a coherent laser beam.

Experimental Results

Deduction of the Imaging Code

The images obtained from the polytypes 6 *O*, 2 *O*, and 4 *M*, all taken under strictly controlled diffraction conditions, can be compared with the corresponding X-ray structures, as shown in Fig. 5. These images, suggest that an *S* block should be imaged as a (mostly bright) parallellogram with a slope corresponding to the Y-planes, described above. The *T* block is imaged as a (mostly darker) parallellogram, also having the same slopes as its Y-planes.

The alteration of *S* and *T* blocks can be clearly resolved, but due to the resolution

limit, the *SSS* and *TTT* blocks are imaged as a single parallellogram of triple length.

Investigation of the Other Polytypes

Using the contrast features revealed by the imaging code, the images of the other five polytypes could be directly translated in terms of *S* and *T* blocks.

As shown in Figs. 6 and 7, the following stacking sequences can be read from the images.

6 *M* *SSSTST*
8 *M* *SSSTSTST*
10 *M* *SSSTSTSTST*
12 *M* *SSSTSTSTSTST*
14 *O* *SSSTSTSTTTSTST*

A schematic representation of the projected structure is separately shown in the same figures. Polytypes consisting of the same stacking combination but for which *S* and *T* were interchanged and polytypes related by the (*a*, *c*) mirror plane can be considered as being the same, due to the symmetry of the S and T blocks.[1]

New Polytypes

A number of new polytypes could be observed in syntaxy with other polytypes as:

14 *M* in 12 *M*;
(10 + 12) *M* in 10 *M*;

[1] The crystal structures of the polytypes 14 *O* and 10 *M* and very recently of the polytype 8 *M* have since also been determined by means of X-ray diffraction, confirming the block sequences revealed by electron microscopy.

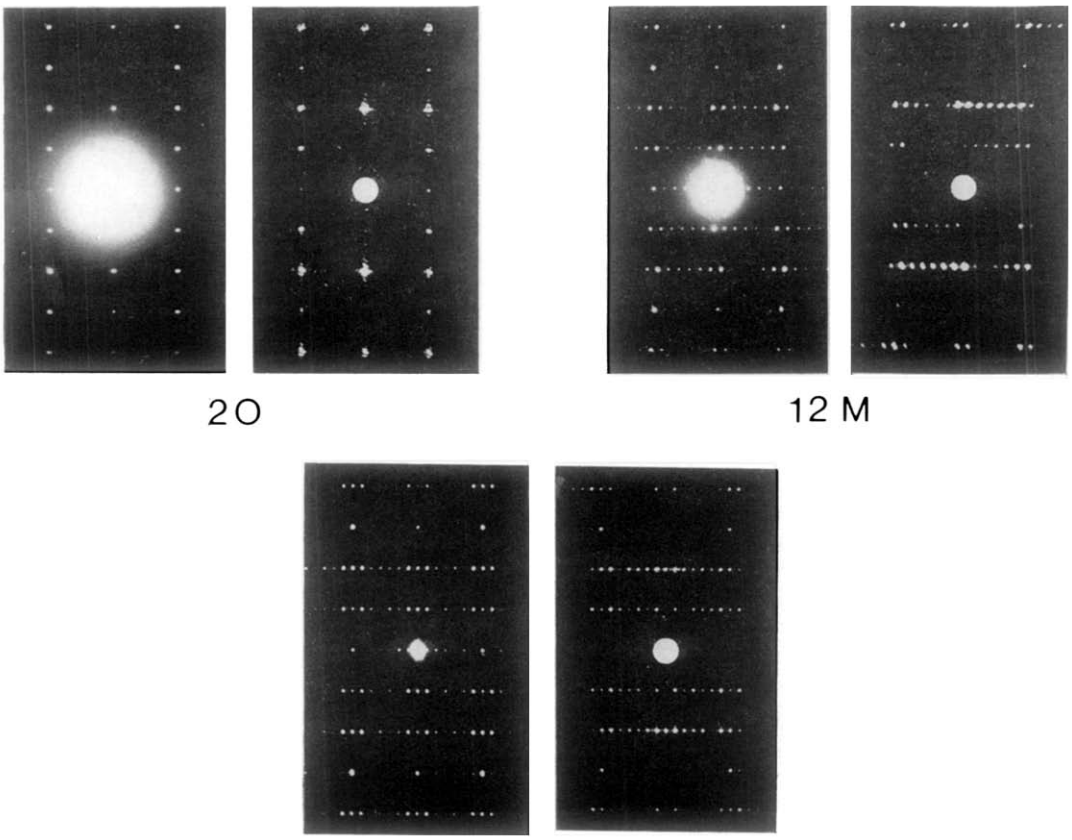

FIG. 10. Comparison between the simulated and the electron diffraction patterns obtained for the different polytypes: 2 *O*, 10 *M*, and 14 *O*.

and

16 *O* in 14 *O*.

For 14 *M*, a direct lattice image could be obtained, as shown in Fig. 7, the stacking sequence of which can be interpreted as: *SSSTSTSTSTSTST*. Although no high-quality images could be produced for the polytype (10 + 12) *M* the micrographs allow one to interpret the structure as consisting of alternating strips, respectively, about 32 and 38 Å wide, as seen in Fig. 8 with a slope corresponding to 10 *M* respectively 12 *M*. This suggests an alternative stacking of the polytypes 10 *M* and 12 *M* which can be represented in symbols as: *SSSTSTSTSTSSSTSTSTSTST*.

TABLE I

Polytype	Sequence	Annealing temperature (°C)
6 *O*	*SSSTTT*	500
2 *O*	*ST*	800
14 *O*	*SSSTSTSTTTSTST*	1030
14 *M*	*SSSTSTSTSTSTST*	
12 *M*	*SSSTSTSTSTST*	
(10+12) *M*	*SSSTSTSTSTSSSTSTSTSTST*	1050
10 *M*	*SSSTSTSTST*	1050
8 *M*	*SSSTSTST*	1080
6 *M*	*SSSTST*	1105
4 *M*	*SSST*	1150

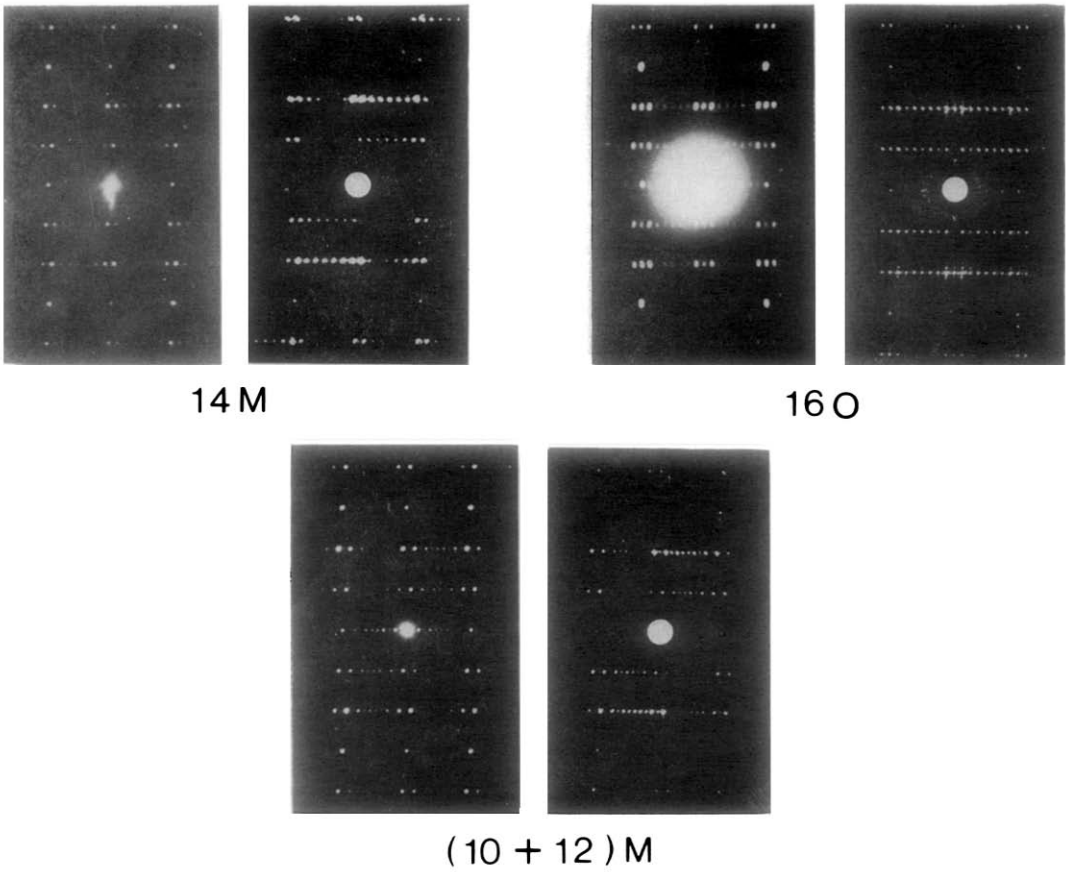

FIG. 11. Comparison between the simulated and the electron diffraction patterns for the polytypes 14 *M*, (10 + 12) *M*, and 16 *O*, which allows us to confirm the proposed stacking sequences.

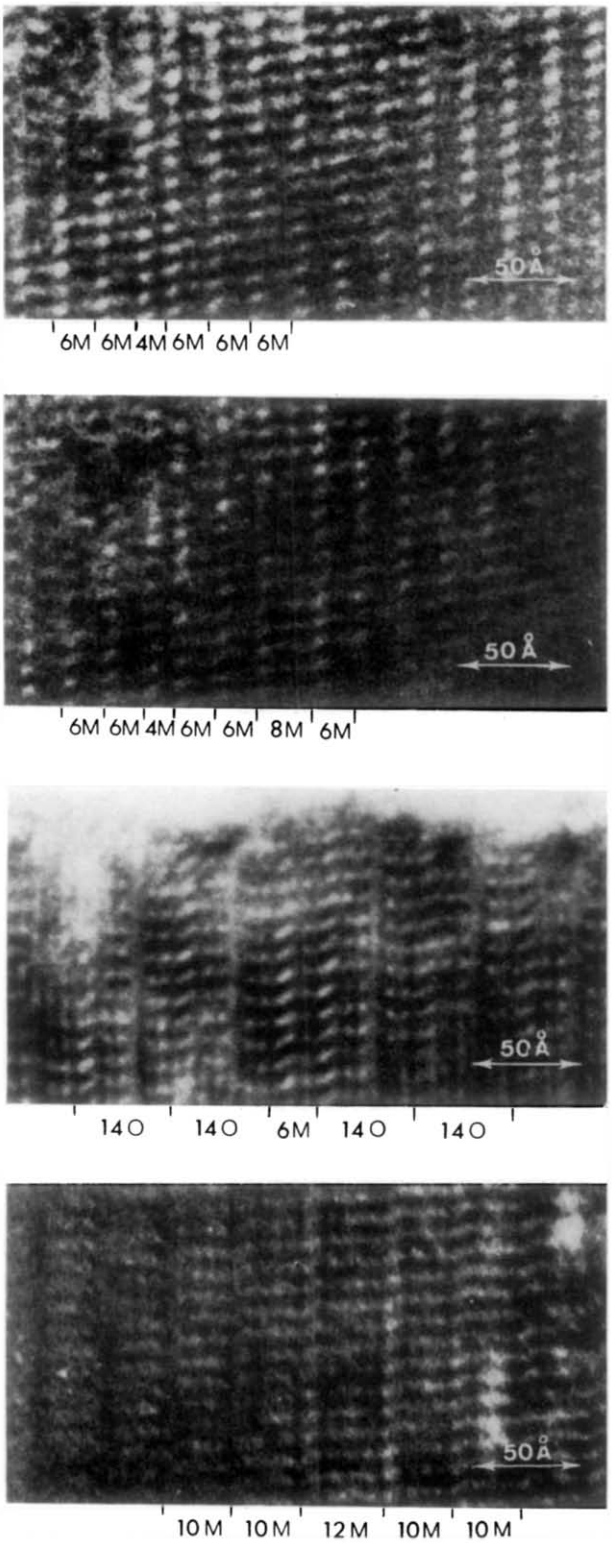

FIG. 12. Examples of polytypic defects, occurring as an intergrowth in a regular matrix.

This proposed stacking sequence was also confirmed by the diffraction simulation, which could also be used for the identification of the new polytype 16 *O*, for which only diffraction patterns could be obtained.

Diffraction Simulation

The technique of optical simulation of the electron diffraction patterns (Fig. 9) was applied for all the polytypes considered above. In spite of the rather crude structure models used to represent the *S* and *T* blocks a remarkable resemblance could be obtained, as can be seen in Fig. 10, where the simulated patterns (right) are compared with the electron diffraction patterns (left).

From the close resemblance of the patterns in Fig. 11, it can be concluded that the proposed sequences for the polytypes 14 *M* and (10 + 12) *M* are justified and that stacking of 16 *O* is likely to be *SSSTSTSTSTTTSTST*. All of the polytypes that could be identified are summarized in Table I with their corresponding stacking sequences and annealing temperatures. It must be noticed that the high-temperature polytypes are all monoclinic and can be described by the repeated occurrence of an *SSS* triad in an *ST* matrix as if a *T* block is transformed into an *S* block at periodic distances. These distances decrease with increasing annealing temperature. If such a transformation would be accompanied by a slight compositional change, the variation in spacing of the triads with temperature might suggest a means of incorporating deviations from stoichiometry in an analogous way as for shear structures so that the description in terms of polytypism becomes questionable. A more detailed investigation at this point is therefore necessary.

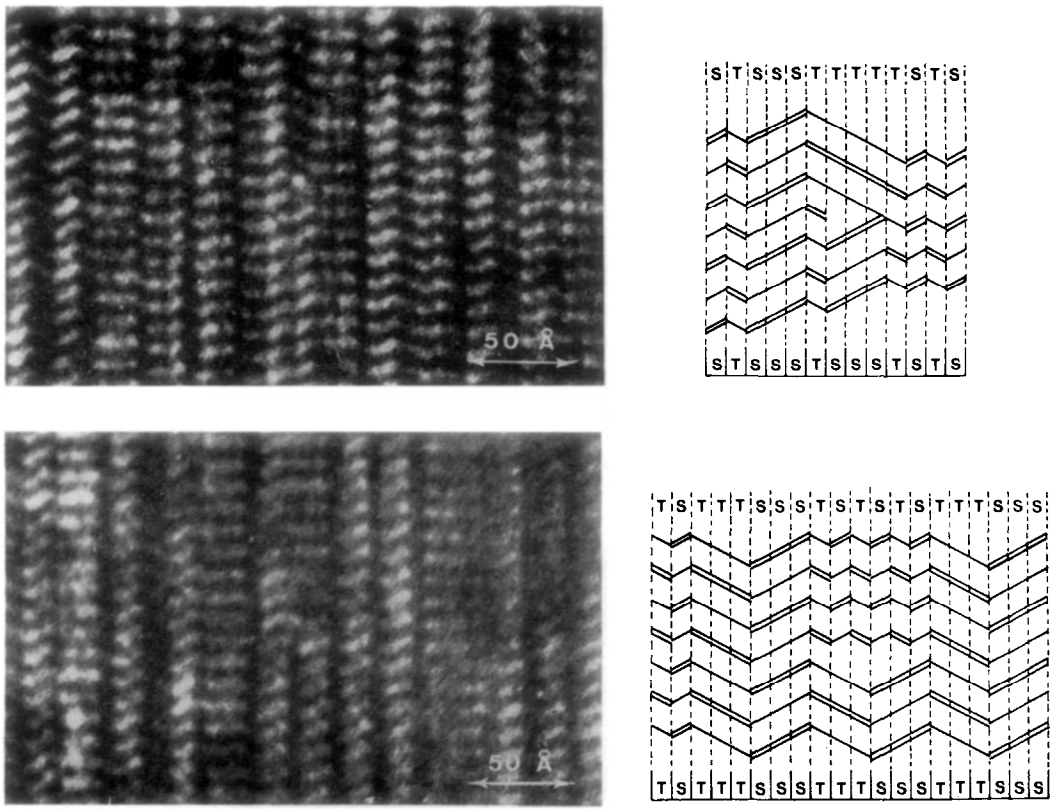

FIG. 13. Two examples of "frozen-in" defects, associated with the polytype growth. The schematized structure and the stacking sequences can be read from the images.

Polytypic Defects

A remarkable feature of the polytypes is their strong tendency to maintain the S and T strips throughout the whole crystal so that most of the observed defects are only sequential. In some of the polytypes they could be imaged and directly interpreted in terms of S and T blocks. Some examples are given in Fig. 12 which can be interpreted, respectively, as

(1) an intergrowth of 4 M in a matrix of 6 M with the sequence

$$\underset{6\,M}{SSSTST}\,|\,\underset{4\,M}{SSST}\,|\,\underset{6\,M}{SSSTST}$$

(2) an intergrowth of 4 M and 8 M in a 6 M matrix with the sequence

$$\underset{6\,M}{SSSTST}\,|\,\underset{4\,M}{SSST}\,|\,\underset{6\,M}{SSSTST}\,|\,\underset{6\,M}{SSSTST}\,|\,\underset{8\,M}{SSSTSTST}\,|\,\underset{6\,M}{SSSTST}$$

This double fault can be described by the displacement of one ST combination so that the matrix at both sides of the fault remains in phase:

(1) an intergrowth of 6 M in a matrix of 14 O given by the sequence

$$\underset{14O}{SSSTSTSTTTSTST}\,|\,\underset{6\,M}{SSSTST}\,|\,\underset{14\,O}{SSSTSTSTTTSTST}$$

(2) an intergrowth of 12 M in the matrix 10 M given by

$$\underset{10\,M}{SSSTSTSTST}\,|\,\underset{12\,M}{SSSTSTSTSTST}\,|\,\underset{10\,M}{SSSTSTSTST}$$

Growth Defects

Only the low-temperature polytype 6 O showed highly faulted regions. In such areas it was possible to image occasionally some growth defects lying along the c-axis and frozen in during their propagation in the a direction.

Two typical examples are given in Fig. 13 together with the proposed transcription into the S- and T-block symbolism.

It is our hope that a more detailed study of such growth defects will give more information about the growth mechanism of the polytypes.

Conclusions

High-resolution electron microscopy was shown to be a useful tool for the study of YSeF polytypism. The previous knowledge about the structure obtained by means of X-ray diffraction could be used to establish an imaging code. In such cases this technique becomes very powerful and more suitable for the study of more complicated sequences. Then, investigations of polycrystalline and disordered stackings can also be carried out.

Optical simulation of the electron diffraction pattern appears to offer a convenient means for checking regular polytypic stacking models, especially in cases where direct imaging is difficult.

In this paper, both techniques were applied to the study of YSeF polytypes which appeared to be formed by the repeated stacking of two kinds of monoclinic blocks S and T. The symmetry of these blocks causes the polytypes to be subdivided into an orthorhombic and a monoclinic class, and their lattice parameters were found to obey simple equations related to the number of the blocks.

Sequences of S and T blocks could be images within the resolution limits of the electron microscope. The model of the polytypism in terms of S and T stacking was shown to be convenient for the description of all the other polytypes. The monoclinic

polytypes can be described by a periodic occurrence of $T \rightarrow S$ transformations at regular distances, inversely related to the annealing temperature. If this transformation were accompanied by compositional changes this could suggest a rather "shear structure"-like formalism mechanism for these compounds.

A number of new types and polytypic defects was discovered and characterized. Direct images of some growth defects could be interpreted. A more detailed study of these defects can probably yield more information about the growth mechanism of the polytypes.

References

1. C. DAGRON, *Comptes Rend. Sér. C* **275**, 817 (1972).
2. N. HUY-DUNG, *Acta Crystallogr.* **B29**, 2095 (1973).
3. N. HUY-DUNG, C. DAGRON, AND P. LARUELLE, *Acta Crystallogr.* **B31**, 514 (1975).
4. N. HUY-DUNG, C. DAGRON, AND P. LARUELLE, *Acta Crystallogr.* **B31**, 519 (1975).